

# Subchondral Drilling Independent of Drill Hole Number Improves Articular Cartilage Repair and Reduces Subchondral Bone Alterations Compared With Debridement in Adult Sheep

Niklas Stachel,\* MD, Patrick Orth,\* MD, David Zurakowski,<sup>†</sup> PhD, Michael D. Menger,<sup>‡</sup> MD, Matthias W. Laschke,<sup>‡</sup> MD, Magali Cucchiari,<sup>\*</sup> PhD, and Henning Madry,<sup>\*,§</sup> MD

*Investigation performed at the Center of Experimental Orthopaedics, Saarland University, Homburg/Saar, Germany*

**Background:** Subchondral drilling is an established marrow stimulation technique for small cartilage defects, but whether drilling is required at all and if the drill hole density affects repair remains unclear.

**Hypotheses:** Osteochondral repair is improved when the subchondral bone is perforated by a higher number of drill holes per unit area, and drilling is superior to defect debridement alone.

**Study Design:** Controlled laboratory study.

**Methods:** Rectangular full-thickness chondral defects (4 × 8 mm) were created in the trochlea of adult sheep (N = 16), debrided down to the subchondral bone plate without further treatment as controls (no treatment; n = 7) or treated with either 2 or 6 (n = 7 each) subchondral drill holes (diameter, 1.0 mm; depth, 10.0 mm). Osteochondral repair was assessed at 6 months postoperatively by standardized (semi-)quantitative macroscopic, histological, immunohistochemical, biochemical, and micro-computed tomography analyses.

**Results:** Compared with defect debridement alone, histological overall cartilaginous repair tissue quality ( $P = .025$ ) and the macroscopic aspect of the adjacent cartilage ( $P \leq .032$ ) were improved after both drilling densities. Only drilling with 6 holes increased type 2 collagen content in the repair tissue compared with controls ( $P = .038$ ). After debridement, bone mineral density was significantly decreased in the subchondral bone plate ( $P \leq .015$ ) and the subarticular spongiosa ( $P \leq .041$ ) compared with both drilling groups. Debridement also significantly increased intralesional osteophyte sectional area compared with drilling ( $P \leq .034$ ). No other differences in osteochondral repair existed between subchondral drilling with 6 or 2 drill holes.

**Conclusion:** Subchondral drilling independent of drill hole density significantly improves structural cartilage repair compared with sole defect debridement of full-thickness cartilage defects in sheep after 6 months. Subchondral drilling also leads to a better reconstitution of the subchondral bone compartment below the defects. Simultaneously, drilling reduced the formation of intralesional osteophytes caused by osseous overgrowth compared with debridement.

**Clinical Relevance:** These results have important clinical implications, as they support subchondral drilling independent of drill hole number but discourage debridement alone for the treatment of small cartilage defects. Clinical studies are warranted to further quantify the effects of subchondral drilling in similar settings.

**Keywords:** marrow stimulation; subchondral drilling; articular cartilage repair; subchondral bone; sheep

Small focal chondral defects are commonly treated with marrow stimulation techniques such as microfracture, subchondral drilling, and abrasion.<sup>12,19,47,50,55</sup> Microfracture

is frequently used because it is applicable to regions with difficult arthroscopic access, it is not associated with possible thermal damage,<sup>32,55</sup> and no undesired breakage of a drill bit by accidentally flexing the device can occur. However, bone impaction<sup>6,35</sup> and confluent holes with unpredictable 3-dimensional (3D) geometry<sup>35</sup> may result from an inaccurate technique and possibly lead to subchondral bone alterations.<sup>37</sup> Subchondral drilling is a cutting process using rotating surgical drill bits or Kirschner (K)



wires<sup>12,47</sup> to create potentially deep cylindrical holes in the debrided<sup>9,11</sup> subchondral bone. Both techniques result in fibrocartilaginous repair,<sup>12,51</sup> while the subchondral bone is remodeled.<sup>41,51</sup> Ian Scott Smilie<sup>53</sup> introduced drilling in 1957 for osteochondritis dissecans, and Kenneth Pridie<sup>47</sup> for osteoarthritis in 1959. Clinical studies report fair short- and midterm results,<sup>3,40,48,50</sup> although no cartilage regeneration occurs.<sup>21,50</sup>

Several preclinical studies have investigated the effect of surgical methodological parameters of the procedure,<sup>12</sup> including the influence of drill hole diameter,<sup>10</sup> drilling depth,<sup>5</sup> debridement,<sup>9,11,15</sup> location,<sup>43</sup> cooled irrigation during drilling,<sup>1,6</sup> cutting device,<sup>6</sup> 3D instrument morphologies,<sup>35</sup> supportive biomaterials,<sup>13,16,18</sup> and adjunctive treatments.<sup>50,56</sup> To the best of our knowledge, the influence of drill hole number on cartilage repair, however, remains unknown. In theory, a higher number of drill holes per unit area may allow for increased access of reparative elements while reducing the stability of the subchondral bone plate, although a causal link has not yet been confirmed.<sup>28</sup> Moreover, whether focal perforations of the subchondral bone plate are required at all remains controversial,<sup>2</sup> since debridement of chondral lesions alone may also provide some access to subchondral sinusoids.<sup>9</sup>

We investigated the effect of drill hole density on osteochondral repair in the knee joint of adult sheep. We first tested the hypothesis that cartilage repair is improved when the subchondral bone plate is perforated with a higher number of drill holes. Second, we tested the hypothesis that subchondral drilling per se is superior to defect debridement alone.

## METHODS

### Study Design

Standardized rectangular full-thickness chondral defects (4 × 8 mm) were created in the lateral trochlea of adult sheep (Figure 1A). In all defects, the entire calcified cartilage layer was debrided down to the subchondral bone plate, which was left intact. Next, standardized subchondral drilling (diameter, 1.0 mm; depth, 10.0 mm) of the debrided defects was performed (Figure 1B) using K-wires applying either a high (6 holes; n = 7 defects) or low (2 holes; n = 7 defects) density of drill holes. Adjusted to the defect area (32.0 mm<sup>2</sup>; 100%), 6 drill holes (each 0.79 mm<sup>2</sup>; total perforated area, 4.71 mm<sup>2</sup>; 15%) represent the maximal number of drill holes that would not lead to unwanted hole confluence respecting a minimum distance of 1.5 to 2.0 mm<sup>31</sup> between individual drill holes. Two drill

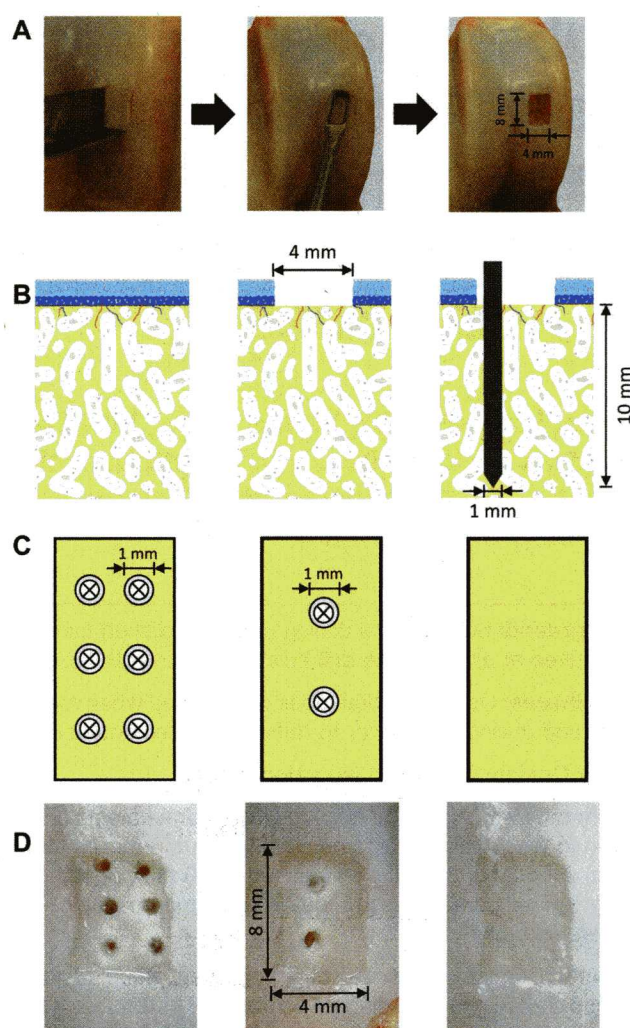


**Figure 1.** (A) Standardized rectangular (4 × 8 mm; 32 mm<sup>2</sup>) full-thickness chondral defects were created in the ovine lateral femoral trochlea with a custom-made, rectangular punch. The defect was debrided down to the subchondral bone with meticulous removal of the entire calcified cartilage layer. Debridement was performed with a clinical rectangular curette. (B) Subsequently, standardized subchondral drill holes (diameter, 1 mm; depth, 10 mm) were introduced perpendicular to the joint surface in the 2 treatment groups using Kirschner wires. Light blue color, hyaline articular cartilage; dark blue color, calcified cartilage; yellow color, subchondral bone; violet line, tidemark; gray line, cement line. (C) Treated defects received 2 or 6 drill holes in a standardized pattern. Controls were identically debrided but did not receive drilling. (D) Intraoperative photographs after treatment.

<sup>§</sup>Address correspondence to Henning Madry, MD, Center of Experimental Orthopaedics, Saarland University, Kirrberger Straße 100, Building 37, Homburg, D-66421, Germany (email: henning.madry@uks.eu).

<sup>\*</sup>Center of Experimental Orthopaedics, Saarland University Medical Center and Saarland University, Homburg/Saar, Germany.

<sup>†</sup>Departments of Anesthesia and Surgery, Boston Children's Hospital, Harvard Medical School, Boston, Massachusetts, USA.

<sup>‡</sup>Institute for Clinical and Experimental Surgery, Saarland University Medical Center and Saarland University, Homburg/Saar, Germany.

Submitted December 2, 2021; accepted April 12, 2022.

One or more of the authors has declared the following potential conflict of interest or source of funding: This study was supported in part by the Gesellschaft fuer Orthopaedisch-Traumatologische Sportmedizin. AOSSM checks author disclosures against the Open Payments Database (OPD). AOSSM has not conducted an independent investigation on the OPD and disclaims any liability or responsibility relating thereto.



holes (total perforated area,  $1.57 \text{ mm}^2$ ) involving only 5% of the defect area were chosen to represent a low drill hole density. A third group of control defects was identically debrided but received no drilling (no treatment;  $n = 7$  defects) (Figure 1C). Treatment and control procedures were randomized by arbitrarily alternating left and right knees. Osteochondral repair was assessed *ex vivo* after sacrifice and sample retrieval by 2 blinded observers (N.S., P.O.) at 6 months postoperatively. Cartilage repair was evaluated by established semiquantitative macroscopic, histological, immunohistochemical scoring, and biochemical analyses. The subchondral bone was analyzed by histological scoring and micro-computed tomography (micro-CT).<sup>10,39,41</sup> A protocol including the research question, key design features, and analysis plan was submitted with the animal application.

### Animal Experiments

All animal experiments were conducted in agreement with the national legislation on protection of animals and the National Institutes of Health (NIH) *Guidelines for the Care and Use of Laboratory Animals* (NIH Publication 85-23; Rev 1985) and were approved by the local governmental animal care committee (20/2011). Skeletally mature, healthy, female Merino sheep ( $n = 17$ ; mean age,  $34 \pm 8$  months; mean ( $\pm$ SD) body weight [BW],  $77.1 \pm 4.4$  kg) received water *ad libitum* and were fed a standard diet. Sample size requirements were calculated based on 80% statistical power using the 2-sample Student *t* test based on comparable previous studies.<sup>10,39,43,44</sup> For the current mixed unilateral/bilateral study design, a sample size of 8 knees per treatment group and 7 knees in the control group (no treatment) was adopted (23 knees, 17 sheep). One sheep was excluded as a consequence of a postoperative joint infection, which was our *a priori* established exclusion criterion. All other animals (21 knee joints, 16 sheep) were included in further analyses. All animals were kept in appropriate stalls and continuously monitored by a veterinarian. After a 12-hour fast, animals were sedated with 1% xylazine administered intramuscularly (Bayer) at 0.05 mg/kg BW and endotracheally intubated after intravenous administration of 30 mL of 1% propofol (AstraZeneca). Anesthesia was maintained by inhalation of 1.5% isoflurane (Baxter) and intravenous administration of propofol (6-20 mg/kg BW/h). Surgical exposure was performed as previously described.<sup>42</sup> Standardized rectangular full-thickness chondral defects ( $n = 21$ ;  $4 \times 8 \text{ mm}$ ;  $32 \text{ mm}^2$ ) were created in the lateral femoral trochlea with a custom-made, rectangular punch (Aesculap) (Figure 1A). The entire calcified cartilage layer was carefully removed down to the subchondral bone plate, which was not abraded (Figure 1A). No bleeding from the exposed subchondral bone plate was observed before subchondral drilling. Either 2 or 6 drill holes (constant diameter, 1.0 mm) were then introduced perpendicular to the joint surface within 14 of 21 defects (2 drill holes, 7 defects; 6 drill holes, 7 defects) using K-wires with a threaded trocar tip driven by a power drill (MBQ 700; De Soutter

Medical Limited) (Figure 1, B and C). A rigid metallic drill sleeve used as drilling stop enabled standardization of the drilling depth (10 mm). Drilling was always performed under constant irrigation (saline) to avoid thermal necrosis. Seven defects did not receive subchondral drilling and served as controls (Figure 1C). In detail, 10 defects treated with either 2 or 6 drill holes were created bilaterally in the same animal (right and left knees alternating between treatment groups;  $n = 10$  defects in 5 animals). The remaining defects treated by subchondral drilling ( $n = 4$ ) as well as all control defects (no treatment;  $n = 7$ ) were created 1-sided in independent animals ( $n = 11$  defects in  $n = 11$  animals). Contralateral joints received cartilage defects through comparable surgical procedures (identical approach and extent of arthrotomy, size, geometry, depth, location of defect, marrow stimulation procedure) in the context of an unpublished study. Joints were closed in layers after thorough rinsing. Hence, all sheep were operated bilaterally and were allowed immediate full weightbearing. No apparent clinical differences in pain or individual joint loading were noted in any of the animals postoperatively.

Postoperatively, 3 mL of 0.25% fentanyl/levomeperidone (MSD) and streptomycin/benzylpenicillin (12/7 mg/kg BW; Albrecht) were applied intramuscularly. Carprofen (1.4 mg/kg BW; Pfizer) was administered daily subcutaneously for 2 weeks.

Animals were sacrificed 6 months postoperatively. Immediately after sacrifice, the defects were photo-documented using standardized illumination conditions.<sup>17</sup> The repair tissue from the proximal halves of the defects ( $4 \times 4 \text{ mm}$ ) and the adjacent articular cartilage within 3 mm directly neighboring the proximal defect borders ( $4 \times 3 \text{ mm}$ ) were retrieved and stored at  $-80^\circ\text{C}$  for biochemical analyses. The remaining osteochondral units were trimmed and stored in 70% ethanol until further analytical processing.

### Evaluations of Articular Cartilage Repair

Based on the photographs of the entire defect area ( $n = 21$ ), macroscopic evaluation of articular cartilage repair was performed by 2 blinded investigators (N.S., P.O.) applying a validated inverse scoring system<sup>17</sup> (20 points, no repair; 0 points, normal articular cartilage). Degenerative changes of the articular cartilage surface adjacent to the distal defect halves were stained with India ink.<sup>27</sup> Osteoarthritis changes were manually measured on digitalized photographs (analySIS 5.0; Olympus Soft Imaging System) within a standardized region of interest (width, 2.5 mm; area,  $42.5 \text{ mm}^2$ ) surrounding the distal defect halves.

For histological evaluation, osteochondral specimens were trimmed, decalcified, dehydrated, and paraffin embedded. Coronal sections ( $4 \mu\text{m}$ ) of the distal defect halves were stained with safranin orange/fast green (safranin O) and hematoxylin and eosin.<sup>36</sup> Osteochondral repair was semiquantitatively graded<sup>49</sup> (31 points, no repair; 0 points, regeneration) on 8 to 10 histological sections per defect taken from the center of the distal defect halves (total



of 176 sections). All histological scoring was performed blinded by 2 independent investigators (N.S., P.O.) (magnification,  $\times 20$  and  $\times 40$ ) using a solid-state CCD camera mounted on a BX-45 light microscope (Olympus).

For immunohistochemical detection of type 1 and 2 collagen, deparaffinized sections were exposed to a 1/90 dilution of a monoclonal mouse anti-type 1 or a 1/45 dilution of a monoclonal mouse anti-type 2 collagen immunoglobulin G (both Acris) and then exposed to a 1/200 dilution of a biotinylated goat anti-mouse immunoglobulin G secondary antibody (Vector Laboratories). Type 1 and 2 collagen immunoreactivities were evaluated on 1 section per defect taken from the center of the distal defect halves, respectively ( $n = 42$  sections). Immunoreactivity to type 1 collagen in the repair tissue was compared with that of the adjacent subchondral bone, serving as a positive internal control (0 points, no immunoreactivity; 1 point, significantly weaker; 2 points, moderately weaker; 3 points, similar; 4 points, stronger immunoreactivity).<sup>38</sup> Immunoreactivity to type 2 collagen in the repair tissue was compared with that of the adjacent articular cartilage applying an identical semiquantitative grading.<sup>38</sup>

Degenerative changes in the adjacent cartilage were graded within 3 mm of the lateral and medial borders of the defect area on 3 safranin O–stained sections per defect (distal, middle, proximal;  $n = 63$  sections) semiquantitatively<sup>24</sup> (25 points, severe degeneration; 0 points, normal cartilage).

For biochemical analyses of the cartilaginous repair tissue (proximal defect halves) and directly adjacent cartilage (within 3 mm of the proximal defect border) ( $n = 21$  samples each), samples were digested for 24 hours in papain solution (0.5 mg/mL; diluted in phosphate-buffered saline) at 60°C to 64°C. The deoxyribonucleic acid (DNA) content was determined by Hoechst 33258 assay.<sup>20</sup> The bicinchoninic acid test was used for detecting the protein content.<sup>54</sup> Proteoglycan concentrations were measured spectrophotometrically by binding to dimethylmethylene blue dye (pH 3.5),<sup>33</sup> while chondroitin-6-sulfate served as standard. All measurements were performed using a spectrophotometer/fluorometer (GENios; Tecan).

### Micro-CT Imaging of the Subchondral Bone

The subchondral bone plate and subarticular spongiosa beneath the cartilage defects (defect areas;  $n = 21$ ), directly adjacent to defects (adjacent areas;  $n = 21$ ), and adjacent to defects with ample distance (normal controls;  $n = 21$ ) were separately assessed using a microfocused radiographic CT scanner (Skyscan 1172; Bruker) with a spatial resolution of 14  $\mu\text{m}$ .<sup>41</sup>

The subchondral bone compartment was segmented into the volumes of interest (VOIs) “subchondral bone plate–defect,” “subchondral bone plate–adjacent,” and “subchondral bone plate–normal,” as well as “subarticular spongiosa–defect,” “subarticular spongiosa–adjacent,” and “subarticular spongiosa–normal” (CTAnalyzer, Skyscan).<sup>41</sup> The VOIs “subchondral bone plate–normal” and “subarticular spongiosa–normal” were placed adjacent to the defect with a minimum

distance of 3.5 mm and served as normal controls. For data presentation, the VOIs “subchondral bone plate–adjacent” and “subarticular spongiosa–adjacent” as well as “subchondral bone plate–normal” and “subarticular spongiosa–normal” of all 3 groups were consolidated, respectively (Appendix Tables A3 and A4, available in the online version of this article). The total depth of all VOIs did not exceed 10 mm, whereas the total width was restricted to 3.5 mm. Overlapping of VOIs was strictly avoided.

The following 3D structural parameters were determined within all VOIs: bone mineral density (BMD), bone volume fraction, bone surface/volume ratio, and bone surface density. Cortical thickness was measured only within the subchondral bone plate, while trabecular thickness, trabecular separation, trabecular pattern factor, trabecular number, structure model index, degree of anisotropy (DA), and fractal dimension were determined only in the subarticular spongiosa.

Measurements of intralesional osteophytes were performed as previously described.<sup>14</sup> Maximum height, base diameter, longitudinal diameter, maximum longitudinal sectional area, and 3D volume were measured and location was reported (central: between drill holes; peripheral: between drill hole and defect border) for all defects ( $n = 21$ ) (CTAnalyzer, Skyscan). Grades of osteophyte overgrowth were determined based on a magnetic resonance imaging grading system,<sup>30</sup> compared with the adjacent cartilage thickness (grade 0, no overgrowth; grade 1, maximal osteophyte height 1%–33% of chondral thickness; grade 2, maximal osteophyte height 34%–66% of thickness; grade 3, maximal osteophyte height  $\geq 67\%$  of thickness).<sup>30</sup> The adjacent cartilage thickness was measured within 3 mm of the respective medial and lateral defect borders on safranin O–stained histological sections ( $n = 2 \times 18$ ).

### Statistical Analysis

In compliance with the Kolmogorov-Smirnov goodness-of-fit test, all data were nonnormally distributed. Data were analyzed using the Kruskal-Wallis  $H$  test to compare all 3 groups for each parameter. The Mann-Whitney  $U$  test was used to compare the individual differences between single groups. Distributions of the respective data are given as mean and 95% CI. Regarding the incidence rates of osteophyte formations, groups were compared using the chi-square test. A  $P$  value  $< .05$  was considered significant. All tests were performed applying the SPSS Statistics software (Version 26.0; IBM).

## RESULTS

### Analyses of Articular Cartilage Repair

Semiquantitative analysis of macroscopic repair<sup>17</sup> (Figure 2A) yielded no significant differences between all groups for all individual parameters ( $P \geq .518$ ) and mean total score value ( $P = .768$ ) (Table 1). Histological grading<sup>49</sup> of the repair tissue (Table 2) revealed that either subchondral



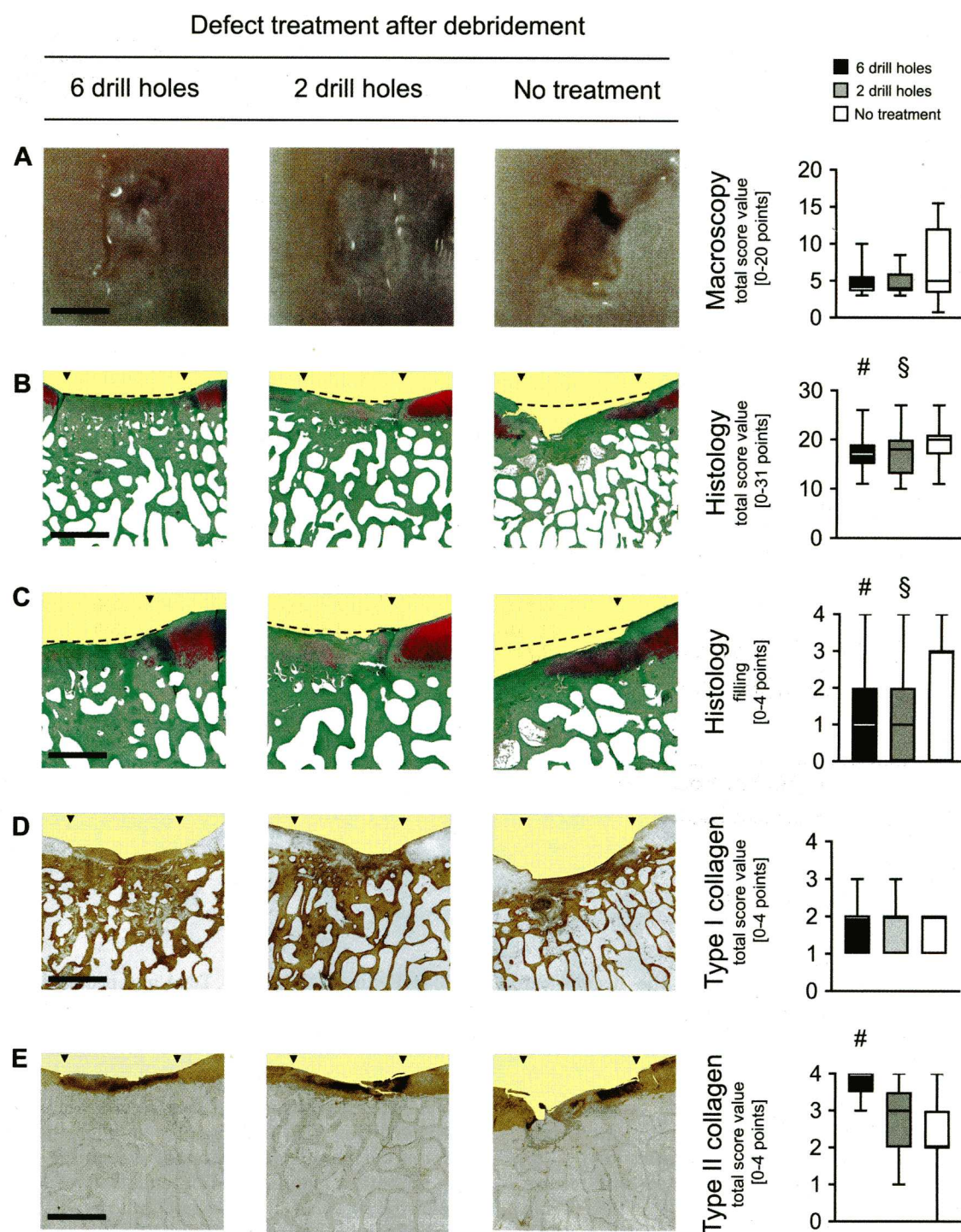


**Figure 2.** (A) Semiquantitative macroscopic analysis of the repair tissue<sup>17</sup> yielded no significant differences between the different treatment groups (6 or 2 drill holes) and the debrided controls (no treatment) for all individual parameters and the mean total score value. (B) Semiquantitative histological grading of the cartilaginous repair tissue according to Sellers et al<sup>49</sup> revealed that either subchondral drilling technique significantly improved the histological total score value compared with debrided defects. (C) Among others, 2 and 6 drill holes improved the single parameter of defect filling compared with debridement. (D) Immunoreactivity for type 1 collagen was not significantly different between all 3 groups. (E) Subchondral drilling by 6 drill holes significantly increased type 2 collagen content compared with debridement. <sup>#</sup>*P* < .05 for 6 drill holes versus debridement; <sup>§</sup>*P* < .05 for 2 drill holes versus debridement. Triangles indicate defect borders. The interrupted lines mark the course of an intact cartilage surface. Scale bars: (A) 4 mm, (B) 2 mm, (C) 1 mm, and (D, E) 2 mm.



TABLE 1  
Semiquantitative Macroscopic Analysis of Articular Cartilage Repair<sup>a</sup>

| Parameter                                    | Defect Treatment After Debridement |                  |                    | P Value <sup>b</sup> |          |
|--|------------------------------------|------------------|--------------------|----------------------|----------|
|  | 6 Drill Holes                      | 2 Drill Holes    | No Treatment       | Overall              | Specific |
| Color of repair tissue                       | 0.6 (0.0 to 1.1)                   | 0.6 (0.2 to 1.1) | 1.5 (-0.2 to 3.2)  | .843                 | ND       |
| Presence of blood vessels                    | 0.7 (0.0 to 1.5)                   | 0.5 (0.0 to 1.0) | 0.4 (-0.2 to 1.00) | .672                 | ND       |
| Surface of repair tissue                     | 1.7 (1.0 to 2.4)                   | 1.5 (0.7 to 2.2) | 2.2 (0.8 to 3.6)   | .591                 | ND       |
| Filling of defect                            | 0.6 (0.4 to 0.9)                   | 0.8 (0.5 to 1.1) | 1.5 (0.2 to 2.8)   | .518                 | ND       |
| Degeneration of adjacent articular cartilage | 1.4 (0.8 to 2.0)                   | 1.6 (0.9 to 2.3) | 1.9 (0.8 to 2.9)   | .632                 | ND       |
| Mean total score                             | 5.0 (2.8 to 7.3)                   | 5.0 (3.1 to 6.8) | 7.5 (2.2 to 12.8)  | .768                 | ND       |

<sup>a</sup>Results are reported as mean (95% CI). Validated grading system<sup>17</sup>: 20 = no repair; 0 = complete regeneration. ND, not determined.

<sup>b</sup>For overall P values, a Kruskal-Wallis H test was performed. For specific P values, Mann-Whitney U tests were performed.

TABLE 2  
Semiquantitative Histological Analysis of Articular Cartilage Repair<sup>a</sup>

| Parameter                    | Defect Treatment After Debridement |                  |                  | P Value <sup>b</sup> |                                       |
|------------------------------|------------------------------------|------------------|------------------|----------------------|---------------------------------------|
|                              | 6 Drill Holes                      | 2 Drill Holes    | No Treatment     | Overall              | Specific                              |
| Filling of defect            | 1.3 (0.9-1.6)                      | 1.4 (1.0-1.7)    | 2.0 (1.6-2.5)    | .048                 | .032 <sup>d</sup> ; .043 <sup>e</sup> |
| Integration of repair tissue | 1.7 (1.5-1.8)                      | 2.0 (1.9-2.2)    | 2.0 (1.8-2.2)    | .009                 | NS                                    |
| Matrix staining              | 3.4 (3.2-3.6)                      | 3.4 (3.2-3.6)    | 2.9 (2.6-3.2)    | .010                 | .012 <sup>d</sup> ; .006 <sup>e</sup> |
| Cellular morphology          | 2.6 (2.4-2.9)                      | 2.5 (2.3-2.8)    | 2.8 (2.4-3.2)    | .536                 | ND                                    |
| Architecture within defect   | 2.2 (1.8-2.6)                      | 2.2 (1.8-2.7)    | 2.8 (2.4-3.3)    | .048                 | .028 <sup>d</sup> ; .036 <sup>e</sup> |
| Architecture of surface      | 2.5 (2.3-2.8)                      | 1.9 (1.7-2.2)    | 2.8 (2.7-2.9)    | <.001                | <.001 <sup>c,e</sup>                  |
| New subchondral bone         | 0.0 (0.0-0.0)                      | 0.1 (0.0-0.2)    | 0.0 (0.0-0.0)    | .010                 | NS                                    |
| Tidemark                     | 4.0 (4.0-4.0)                      | 4.0 (4.0-4.0)    | 4.0 (4.0-4.0)    | >.99                 | ND                                    |
| Mean total score             | 17.7 (16.7-18.6)                   | 17.5 (16.5-18.5) | 19.3 (18.0-20.7) | .025                 | .009 <sup>d</sup> ; .033 <sup>e</sup> |

<sup>a</sup>Results are reported as mean (95% CI). Grading system according to Sellers et al<sup>49</sup>: 31 = no repair; 0 = complete regeneration. ND, not determined; NS, no significance.

<sup>b</sup>For overall P values, a Kruskal-Wallis H test was performed. For specific P values, Mann-Whitney U tests were performed.

<sup>c</sup>P < .05 for 6 drill holes versus 2 drill holes.

<sup>d</sup>P < .05 for 6 drill holes versus no treatment.

<sup>e</sup>P < .05 for 2 drill holes versus no treatment.

drilling technique significantly improved the histological total score value compared with only debrided defects (no treatment) ( $P \leq .033$ ) (Figure 2B). Both 2 and 6 drill holes significantly improved the parameter "filling of the defect" ( $P \leq .043$ ) (Figure 2C). Any drilling procedure also significantly enhanced the individual parameter "architecture within defect" ( $P \leq .036$ ) while significantly decreasing matrix staining compared with untreated defects ( $P \leq .012$ ) (Table 2). Two drill holes significantly improved "architecture of surface" compared with untreated defects ( $P < .001$ ) (Table 2). When comparing 2 drill holes with 6 drill holes, the drill hole number had no significant influence on the overall histological outcome of the repair tissue ( $P \geq .774$ ), although 2 drill holes significantly improved architecture of surface compared with 6 drill holes ( $P < .001$ ).

Subchondral drilling by 6 holes significantly increased the type 2 collagen content (Figure 2E) of the repair tissue compared with untreated defects ( $P = .038$ ) (Table 3). No significant differences were observed between the other groups ( $P \geq .103$ ). Immunoreactivity for type 1 collagen was not significantly different between all groups ( $P \geq$

.664) (Figure 2D, Table 3). DNA and proteoglycan contents of the repair tissue and the adjacent cartilage were not significantly different between 2 and 6 drill holes and untreated defects ( $P \geq .073$  and  $P \geq .297$ , respectively) (Appendix Table A1, available online).

Adjacent to the defects, the area affected by macroscopic osteoarthritis was significantly smaller in both drilling groups compared with untreated defects ( $P \leq .032$ ) (Table 4), without a significant difference between 2 and 6 drill holes ( $P = .421$ ). Histological scoring of osteoarthritis revealed no significant differences between the groups for individual parameters ( $P \geq .074$ ) and the mean total score ( $P = .743$ ) except for a significantly increased cluster formation when 6 drill holes were compared with both other groups ( $P \leq .023$ ) (Appendix Table A2, available online).

#### Microstructural Analyses of the Subchondral Bone

In the subchondral bone plate beneath the defects, debridement significantly decreased the BMD compared with 2 and 6 drill holes ( $P \leq .015$ ). Bone volume fraction ( $P =$



TABLE 3  
Semiquantitative Analysis of the Immunoreactivities for Type 1 and 2 Collagen Within the Cartilaginous Repair Tissue<sup>a</sup>

| Parameter       | Defect Treatment After Debridement |               |               | Specific <i>P</i> Value <sup>b</sup> |
|-----------------|------------------------------------|---------------|---------------|--------------------------------------|
|                 | 6 Drill Holes                      | 2 Drill Holes | No Treatment  |                                      |
| Type 1 collagen | 1.9 (1.2-2.5)                      | 1.9 (1.2-2.5) | 1.6 (0.9-2.3) | NS                                   |
| Type 2 collagen | 3.7 (3.3-4.2)                      | 2.7 (1.7-3.7) | 2.2 (0.4-4.0) | .038 <sup>c</sup>                    |

<sup>a</sup>Results are reported as mean (95% CI). Immunoreactivity for type 1 collagen was semiquantitatively compared with adjacent subchondral bone<sup>38</sup>: 0 = no immunoreactivity; 4 = stronger immunoreactivity than in the subchondral bone. Immunoreactivity for type 2 collagen was semiquantitatively compared with adjacent articular cartilage<sup>38</sup>: 0 = no immunoreactivity; 4 = stronger immunoreactivity than in the adjacent articular cartilage. NS, no significance.

<sup>b</sup>For specific *P* values, Mann-Whitney *U* tests were performed.

<sup>c</sup>*P* < .05 for 6 drill holes versus no treatment.

TABLE 4  
Quantitative Analysis of Macroscopic Degenerative Changes Within the Adjacent Articular Cartilage<sup>a</sup>

| Parameter             | Defect Treatment After Debridement |               |               | Specific <i>P</i> Value <sup>b</sup>  |
|-----------------------|------------------------------------|---------------|---------------|---------------------------------------|
|                       | 6 Drill Holes                      | 2 Drill Holes | No Treatment  |                                       |
| Area, mm <sup>2</sup> | 3.0 (1.9-4.0)                      | 2.4 (0.6-4.3) | 5.9 (3.3-8.4) | .032 <sup>c</sup> ; .016 <sup>d</sup> |

<sup>a</sup>Results are reported as mean (95% CI). The articular cartilage surface adjacent to the defects was stained with India ink.<sup>27</sup> Areas with osteoarthritic changes within a standardized region of interest (width, 3.5-4.0 mm; area, 70 mm<sup>2</sup>) surrounding the defect were quantified.

<sup>b</sup>For specific *P* values, Mann-Whitney *U* tests were performed.

<sup>c</sup>*P* < .05 for 6 drill holes versus no treatment.

<sup>d</sup>*P* < .05 for 2 drill holes versus no treatment.

.002), bone surface density ( $P \leq .015$ ), and cortical thickness ( $P \leq .007$ ) were significantly reduced in all groups compared with a normal subchondral bone plate. No other significant differences were detected ( $P \geq .699$ ) (Appendix Table A3, available online). In the subarticular spongiosa beneath the defects, BMD was also significantly reduced after debridement compared with both drilling treatments ( $P \leq .041$ ) and the normal subarticular spongiosa ( $P = .023$ ) (Appendix Table A4, available online). Trabecular thickness was significantly decreased after the application of 2 and 6 drill holes ( $P \leq .048$ ) compared with no treatment. Fractal dimension of the subarticular spongiosa was significantly lower after debridement compared with both drilling groups ( $P \leq .006$ ) and normal controls ( $P = .001$ ). All groups showed a significantly decreased DA compared with the normal subarticular spongiosa ( $P < .001$ ). Two drill holes significantly increased bone surface density ( $P = .041$ ) and structure model index ( $P = .024$ ) compared with normal controls. No significant differences in other parameters were detected ( $P \geq .310$ ).

In the subarticular spongiosa adjacent to the defects, DA was significantly decreased compared with normal controls in all 3 groups ( $P \leq .037$ ) and fractal dimension was reduced after debridement when compared with normal controls ( $P = .048$ ) and with 2-drill hole treatment ( $P = .036$ ) (Appendix Table A4, available online). For all other single parameters, no significant differences existed within the adjacent subchondral bone plate ( $P \geq .078$ ) (Appendix Table A3, available online) and subarticular spongiosa

( $P \geq .095$ ) (Appendix Table A4, available online) between all groups and compared with normal controls.

### Investigation of Intralesional Osteophytes

Intralesional osteophytes emerged in all groups (Figure 3, Table 5). Osteophytes in solely debrided defects were considerably larger and occupied a greater maximum longitudinal sectional area than in both drilling groups. In these untreated defects, osteophyte volume was ~40-fold increased when compared with defects receiving 6 drill holes and ~15-fold increased when compared with defects receiving 2 drill holes. Maximum osteophyte area (~12-fold and ~4-fold, respectively), osteophyte height (~2-fold and ~1.5-fold, respectively), and osteophyte diameters (~8-fold and 5-fold, respectively) were all higher in untreated defects compared with defects receiving either 6 or 2 drill holes. Differences in maximum longitudinal osteophyte sectional area (Figure 3) between control defects and defects in both drilling groups were significant ( $P \leq .034$ ). Maximum base ( $P = .017$ ) and longitudinal diameter ( $P = .030$ ) of intralesional osteophytes were significantly different between control defects and defects receiving 6 drill holes (Table 5). No differences in these parameters were detected between defects receiving 2 or 6 drill holes ( $P \geq .164$ ), and no significant differences existed between all single groups concerning grade of overgrowth ( $P \geq .804$ ).



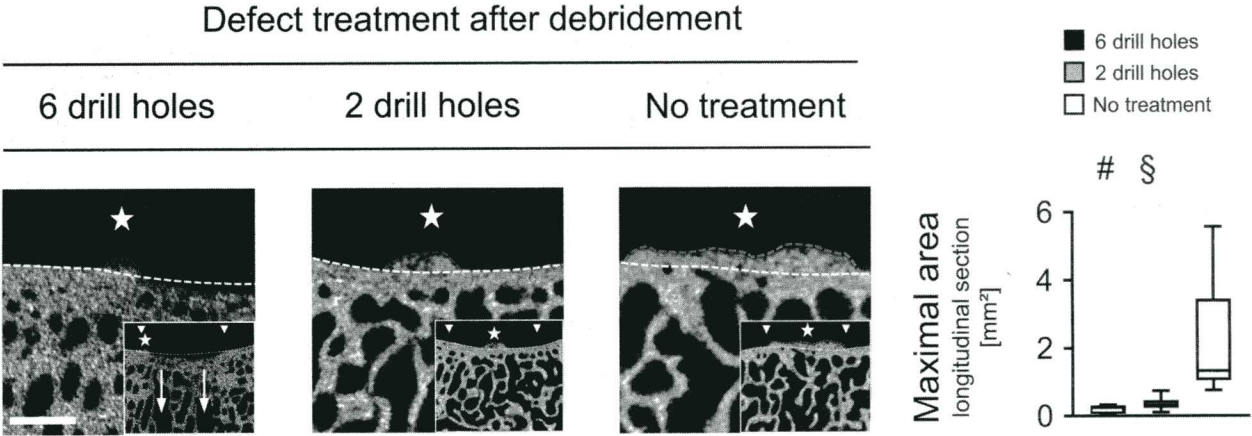


**Figure 3.** Intralesional osteophytes (white stars) were identified in both drilling groups and in debrided defects. Debridement (no treatment) increased maximal longitudinal osteophyte sectional area compared with both drill hole groups. Insets illustrate the osteophyte location within the defects. White triangles denote defect borders; white arrows indicate residual subchondral drill holes and their direction. Interrupted white lines mark the supposed course of the normal subchondral bone plate. Interrupted red lines mark the maximal longitudinal extension of an intralesional osteophyte. The areas between the interrupted white and red lines represent the maximal longitudinal osteophyte sectional areas. <sup>#</sup>*P* < .05 for 6 drill holes versus debridement; <sup>§</sup>*P* < .05 for 2 drill holes versus debridement. Scale bars: 1 mm (insets: 3 mm).

**TABLE 5**  
Quantification of Intralesional Osteophytes Within the Cartilaginous Repair Tissue<sup>a</sup>

| Parameter   | Defect Treatment After Debridement |                  |                   | Specific <i>P</i> Value <sup>b</sup>  |
|---|------------------------------------|------------------|-------------------|---------------------------------------|
|   | 6 Drill Holes                      | 2 Drill Holes    | No Treatment      |                                       |
| Total No.   | 7                                  | 4                | 3                 | ND                                    |
| Incidence, %  | 66.7                               | 50.0             | 50.0              | NS                                    |
| No. per defect  | 1.00 (0.00-3.00)                   | 0.50 (0.00-2.00) | 0.50 (0.00-1.00)  | NS                                    |
| Maximal longitudinal sectional area, mm <sup>2</sup>    | 0.11 (0.03-0.33)                   | 0.32 (0.11-0.74) | 1.33 (0.76-5.57)  | .016 <sup>c</sup> ; .034 <sup>d</sup> |
| Total volume, mm <sup>3</sup>                           | 0.05 (0.01-0.55)                   | 0.16 (0.05-1.90) | 2.42 (0.27-20.22) | NS                                    |
| Maximal height, mm                                      | 0.21 (0.14-0.42)                   | 0.27 (0.20-0.35) | 0.35 (0.32-1.29)  | NS                                    |
| Maximal base diameter, mm                               | 0.68 (0.25-2.19)                   | 1.15 (0.65-4.29) | 5.80 (3.95-6.18)  | .017 <sup>c</sup>                     |
| Maximal longitudinal diameter, mm                       | 0.68 (0.12-4.19)                   | 1.14 (0.57-3.71) | 4.79 (3.38-5.06)  | .030 <sup>c</sup>                     |
| Grade of overgrowth                                     | 0.89 (0.43-1.35)                   | 1.00 (0.00-2.00) | 1.00 (0.00-3.00)  | NS                                    |
| Number at peripheral/central location within the defect | 4/3                                | 3/1              | 0/3               | ND                                    |

<sup>a</sup>Results are reported as mean (95% CI) unless noted otherwise. ND, not determined; NS, no significance.  
<sup>b</sup>Chi-square tests were used to compare the incidence rates of osteophyte formation. For remaining specific *P* values, Mann-Whitney *U* tests were performed.  
<sup>c</sup>*P* < .05 for 6 drill holes versus no treatment.  
<sup>d</sup>*P* < .05 for 2 drill holes versus no treatment.

**DISCUSSION**

Our data make 2 essential contributions that expand our understanding about the effect of subchondral drilling on the repair of small full-thickness defects. The first major finding is that drilling, independent of drill hole density, significantly improves articular cartilage repair compared with untreated defects. Interestingly, only subchondral drilling at higher density significantly increased type 2 collagen content in the cartilaginous repair tissue compared with untreated defects. The second major finding is the significant negative effect of defect debridement alone on the

microstructure of the subchondral bone within the defect and intralesional osteophyte growth. Here, the BMDs of both the subchondral bone plate and subarticular spongiosa in debrided defects were reduced in comparison with both drill hole groups and normal controls. Moreover, the maximum longitudinal sectional area of intralesional osteophytes—a surrogate of intralesional osteophyte size—in untreated defects was significantly increased compared with both drilling groups.  
Recruitment of mesenchymal stromal cells (MSCs) by subchondral drilling improves osteochondral repair.<sup>5,7</sup> Our observation that drilling of debrided cartilage defects



significantly improved structural cartilage repair may be attributed to a better defect filling and architecture, possibly increasing durability of the repair tissue. Besides, its increased volume and quality may better protect the adjacent cartilage, reflected in the reduced areas with perifocal osteoarthritis. In addition, the significantly increased type 2 collagen content after drilling with higher density compared with debridement indicates a superior and more hyaline-like differentiation of the repair tissue<sup>52</sup> and may be linked to enhanced MSC migration and activation.<sup>25,51</sup> Drilling induced superior fibrocartilaginous repair<sup>5,6,10,16,18,23,43</sup> compared with untreated or debrided chondral defects,<sup>16,18,23</sup> although the subchondral bone was not analyzed in these studies. In rats after 4 weeks, drilling improved fibrocartilaginous repair versus debridement (5 drill holes: diameter, 0.2 mm; defect area, 3.1 mm<sup>2</sup>).<sup>18</sup> In goats (unknown drill hole number: diameter, 1 mm; defect area, 28.3 mm<sup>2</sup>) at 4 months postoperatively, drilling improved overall histological score and increased defect filling compared with debrided defects.<sup>23</sup> In sheep, drilling (3 drill holes: diameter, 1.5 mm; defect area, 28.3 mm<sup>2</sup>) led to a complete filling of the defects at 1 year, whereas repair tissue in debrided defects did not sufficiently fill the lesions.<sup>16</sup> A previous ovine study reported enhanced osteochondral repair at 6 months postoperatively after introducing small (diameter, 1.0 mm) compared with larger (diameter, 1.8 mm, both 6 holes) drill holes.<sup>10</sup> The current study was adapted toward this design to allow for comparable conditions. While the first major finding of cartilage repair tissue quality independent of drill hole number (no major differences in osteochondral repair between 6 or 2 drill holes) considerably expands these previous data and also indicates that the subchondral bone plate must be perforated after debridement, an additional spotlight is placed on subchondral alterations and intralesional osteophytes.

The second key finding that extended subchondral bone changes after defect debridement is also clinically relevant. Such alterations are a common and potentially serious<sup>14,55</sup> problem after marrow stimulation, seen in one-third of treated patients<sup>8,22,30,31,48</sup> and in preclinical models.<sup>4,11,14,37,39,41</sup> The osseous repair of drill holes follows a defined bone remodeling sequence usually resulting in incomplete reconstitution of the normal subchondral bone microstructure<sup>6,10,41</sup> and in morphological alterations.<sup>14,15</sup> Interestingly, we observed similar processes in the subchondral bone plate (decreased BMD, bone volume fraction, increased bone surface/volume ratio) and subarticular spongiosa (decreased BMD, DA, fractal dimension) even after sole debridement compared with normal controls. The diminished quantity of mineral as indicated by the reduced BMD may potentially reduce subchondral bone strength, which is also determined by other material and structural properties. Independent of treatment, intralesional osteophytes appeared with incidence rates ranging from 50% to 67% of defects. Of note, drilling with 6 and 2 drill holes generated smaller intralesional osteophytes compared with debridement. Possibly, the superior cartilaginous repair after drilling may afford an improved protection of the

subchondral bone. The enhanced planar migration of the subchondral bone plate caused by the larger osteophytes after debridement may result in an increased degeneration of the thinner cartilaginous repair tissue and the adjacent cartilage. Such subchondral bone changes including intralesional osteophytes possibly deteriorate long-term results of marrow stimulation by disturbing the functional integrity of the osteochondral unit.<sup>8,14,29,30,37,55</sup> In sum, drilling reduced potentially detrimental effects on the subchondral bone compared with debridement as indicated by a more physiological BMD and smaller osteophytes.

The limitations of the current study included that animals were allowed to fully bear weight postoperatively (leading to higher biomechanical stresses than in patients), the midterm time point warranting long-term follow-up, and the testing of only 1 parameter of hole size (diameter, 1.0 mm) and depth (10.0 mm) standardized for both treatment groups based on previous results.<sup>5,10</sup> The potential difference in postoperative pain between bilateral and 1-sided operated animals may theoretically influence postoperative joint loading and osteochondral repair, although all animals always received comparable surgical procedures bilaterally. The strengths are the large animal model, the comprehensive quantification of osteochondral repair by a variety of standardized methods at high detail, and defect location reflecting clinical repair characteristics of the human medial femoral condyle<sup>22,43</sup> where chondral lesions are most frequently located,<sup>57</sup> considering anatomical<sup>26</sup> and biomechanical<sup>46</sup> differences between human and ovine knee joints. The defect size (32 mm<sup>2</sup>) is comparable with a small human defect (~1.3 cm<sup>2</sup>)<sup>10,41,45</sup> considering the distal femoral bicondylar and trochlear widths of humans and sheep (size factor, ~2:1).<sup>34,45</sup>

## CONCLUSION

These translational data support subchondral drilling independent of drill hole number but discourage debridement alone for small full-thickness cartilage defects. Drilling leads to a better reconstitution of the subchondral bone below the defects. Subchondral drilling also reduced the formation of intralesional osteophytes caused by osseous overgrowth compared with debridement alone. Whether these findings are applicable to patients remains to be investigated.

## REFERENCES

1. Augustin G, Davila S, Udiljak T, Staroveski T, Brezak D, Babic S. Temperature changes during cortical bone drilling with a newly designed step drill and an internally cooled drill. *Int Orthop*. 2012;36(7):1449-1456.
2. Bert JM. Abandoning microfracture of the knee: has the time come? *Arthroscopy*. 2015;31(3):501-505.
3. Bouwmeester PSJM, Kuijjer R, Homminga GN, Bulstra SK, Geesink RGT. A retrospective analysis of two independent prospective cartilage repair studies: autogenous perichondrial grafting versus subchondral drilling 10 years post-surgery. *J Orthop Res*. 2002;20(2):267-273.



4. Chen H, Chevrier A, Hoemann CD, Sun J, Ouyang W, Buschmann MD. Characterization of subchondral bone repair for marrow-stimulated chondral defects and its relationship to articular cartilage resurfacing. *Am J Sports Med*. 2011;39(8):1731-1740.
5. Chen H, Hoemann CD, Sun J, et al. Depth of subchondral perforation influences the outcome of bone marrow stimulation cartilage repair. *J Orthop Res*. 2011;29(8):1178-1184.
6. Chen H, Sun J, Hoemann CD, et al. Drilling and microfracture lead to different bone structure and necrosis during bone-marrow stimulation for cartilage repair. *J Orthop Res*. 2009;27(11):1432-1438.
7. Chevrier A, Hoemann CD, Sun J, Buschmann MD. Chitosan-glycerol phosphate/blood implants increase cell recruitment, transient vascularization and subchondral bone remodeling in drilled cartilage defects. *Osteoarthritis Cartilage*. 2007;15(3):316-327.
8. Cole BJ, Farr J, Winalski CS, et al. Outcomes after a single-stage procedure for cell-based cartilage repair: a prospective clinical safety trial with 2-year follow-up. *Am J Sports Med*. 2011;39(6):1170-1179.
9. Drobic M, Radosavljevic D, Cór A, Brittberg M, Strazar K. Debridement of cartilage lesions before autologous chondrocyte implantation by open or transarthroscopic techniques: a comparative study using post-mortem materials. *J Bone Joint Surg Br*. 2010;92(4):602-608.
10. Eldracher M, Orth P, Cucchiari M, Pape D, Madry H. Small subchondral drill holes improve marrow stimulation of articular cartilage defects. *Am J Sports Med*. 2014;42(11):2741-2750.
11. Frisbie DD, Morisset S, Ho CP, Rodkey WG, Steadman JR, McIlwraith CW. Effects of calcified cartilage on healing of chondral defects treated with microfracture in horses. *Am J Sports Med*. 2006;34(11):1824-1831.
12. Gao L, Goebel LKH, Orth P, Cucchiari M, Madry H. Subchondral drilling for articular cartilage repair: a systematic review of translational research. *Dis Model Mech*. 2018;11(6):DMM034280.
13. Gao L, Orth P, Cucchiari M, Madry H. Effects of solid acellular type-I/III collagen biomaterials on in vitro and in vivo chondrogenesis of mesenchymal stem cells. *Expert Rev Med Devices*. 2017;14(9):717-732.
14. Gao L, Orth P, Goebel LK, Cucchiari M, Madry H. A novel algorithm for a precise analysis of subchondral bone alterations. *Sci Rep*. 2016;6:1-12.
15. Gao L, Orth P, Müller-Brandt K, Goebel LKH, Cucchiari M, Madry H. Early loss of subchondral bone following microfracture is counteracted by bone marrow aspirate in a translational model of osteochondral repair. *Sci Rep*. 2017;7:1-16.
16. Giordano M, Aulisa AG, Mastantuoni G, Gigante A, Guzzanti V. Pridie's marrow stimulation technique combined with collagen matrix for cartilage repair. A study in a still growing sheep model. *Int J Immunopathol Pharmacol*. 2011;24(1 suppl 2):101-106.
17. Goebel L, Orth P, Müller A, et al. Experimental scoring systems for macroscopic articular cartilage repair correlate with the MOCART score assessed by a high-field MRI at 9.4 T—comparative evaluation of five macroscopic scoring systems in a large animal cartilage defect model. *Osteoarthritis Cartilage*. 2012;20(9):1046-1055.
18. Hamanishi M, Nakasa T, Kamei N, Kazusa H, Kamei G, Ochi M. Treatment of cartilage defects by subchondral drilling combined with covering with atelocollagen membrane induces osteogenesis in a rat model. *J Orthop Sci*. 2013;18(4):627-635.
19. Johnson LL. Arthroscopic abrasion arthroplasty historical and pathologic perspective: present status. *Arthroscopy*. 1986;2(1):54-69.
20. Kim YJ, Sah RLY, Doong JYH, Grodzinsky AJ. Fluorometric assay of DNA in cartilage explants using Hoechst 33258. *Anal Biochem*. 1988;174(1):168-176.
21. Kraeutler MJ, Aliberti GM, Scillia AJ, McCarty EC, Mulcahey MK. Microfracture versus drilling of articular cartilage defects: a systematic review of the basic science evidence. *Orthop J Sports Med*. 2020;8(8):2325967120945313.
22. Kreuz PC, Steinwachs MR, Erggelet C, et al. Results after microfracture of full-thickness chondral defects in different compartments in the knee. *Osteoarthritis Cartilage*. 2006;14(11):1119-1125.
23. Lind M, Larsen A, Clausen C, Østher K, Everland H. Cartilage repair with chondrocytes in fibrin hydrogel and MPEG polylactide scaffold: an in vivo study in goats. *Knee Surg Sports Traumatol Arthrosc*. 2008;16(7):690-698.
24. Little CB, Smith MM, Cake MA, Read RA, Murphy MJ, Barry FP. The OARS histopathology initiative—recommendations for histological assessments of osteoarthritis in sheep and goats. *Osteoarthritis Cartilage*. 2010;18(suppl 3):80-92.
25. Madry H, Gao L, Eichler H, Orth P, Cucchiari M. Bone marrow aspirate concentrate-enhanced marrow stimulation of chondral defects. *Stem Cells Int*. 2017;2017:1-13.
26. Martini L, Fini M, Giavaresi G, Giardino R. Sheep model in orthopedic research: a literature review. *Comp Med*. 2001;51(4):292-299.
27. Meachim G. Light microscopy of Indian ink preparations of fibrillated cartilage. *Ann Rheum Dis*. 1972;31(6):457-464.
28. Min BH, Choi WH, Lee YS, et al. Effect of different bone marrow stimulation techniques (BSTs) on MSCs mobilization. *J Orthop Res*. 2013;31(11):1814-1819.
29. Minas T, Gomoll AH, Rosenberger R, Royce RO, Bryant T. Increased failure rate of autologous chondrocyte implantation after previous treatment with marrow stimulation techniques. *Am J Sports Med*. 2009;37(5):902-908.
30. Mithoefer K, Venugopal V, Manaqibwala M. Incidence, degree, and clinical effect of subchondral bone overgrowth after microfracture in the knee. *Am J Sports Med*. 2016;44(8):2057-2063.
31. Mithoefer K, Williams RJ, Warren RF, et al. The microfracture technique for the treatment of articular cartilage lesions in the knee: a prospective cohort study. *J Bone Joint Surg Am*. 2005;87(9):1911-1920.
32. Montgomery SR, Foster BD, Ngo SS, et al. Trends in the surgical treatment of articular cartilage defects of the knee in the United States. *Knee Surg Sports Traumatol Arthrosc*. 2014;22(9):2070-2075.
33. Müller G, Hanschke M. Quantitative and qualitative analyses of proteoglycans in cartilage extracts by precipitation with 1,9-dimethylmethylene blue. *Connect Tissue Res*. 1996;33(4):243-248.
34. Oláh T, Cai X, Michaelis JC, Madry H. Comparative anatomy and morphology of the knee in translational models for articular cartilage disorders. Part I: large animals. *Ann Anat*. 2021;235:151680.
35. Onken T, Gao L, Orth P, et al. Investigation of microstructural alterations of the human subchondral bone following microfracture penetration reveals effect of three-dimensional device morphology. *Clin Transl Med*. 2020;10(8):e230.
36. Orth P, Cucchiari M, Kaul G, et al. Temporal and spatial migration pattern of the subchondral bone plate in a rabbit osteochondral defect model. *Osteoarthritis Cartilage*. 2012;20(10):1161-1169.
37. Orth P, Cucchiari M, Kohn D, Madry H. Alterations of the subchondral bone in osteochondral repair—translational data and clinical evidence. *Eur Cell Mater*. 2013;25:299-316.
38. Orth P, Cucchiari M, Zurakowski D, Menger MD, Kohn DM, Madry H. Parathyroid hormone 1-34 improves articular cartilage surface architecture and integration and subchondral bone reconstitution in osteochondral defects in vivo. *Osteoarthritis Cartilage*. 2013;21(4):614-624.
39. Orth P, Duffner J, Zurakowski D, Cucchiari M, Madry H. Small-diameter awls improve articular cartilage repair after microfracture treatment in a translational animal model. *Am J Sports Med*. 2016;44(1):209-219.
40. Orth P, Gao L, Madry H. Microfracture for cartilage repair in the knee: a systematic review of the contemporary literature. *Knee Surg Sports Traumatol Arthrosc*. 2020;28(3):670-706.
41. Orth P, Goebel L, Wolfram U, et al. Effect of subchondral drilling on the microarchitecture of subchondral bone: analysis in a large animal model at 6 months. *Am J Sports Med*. 2012;40(4):828-836.
42. Orth P, Madry H. A low morbidity surgical approach to the sheep. *BMC Musculoskelet Disord*. 2013;14:5. doi:10.1186/1471-2474-14-5.
43. Orth P, Meyer HL, Goebel L, et al. Improved repair of chondral and osteochondral defects in the ovine trochlea compared with the medial condyle. *J Orthop Res*. 2013;31(11):1772-1779.
44. Orth P, Zurakowski D, Alini M, Cucchiari M, Madry H. Reduction of sample size requirements by bilateral versus unilateral research designs in animal models for cartilage tissue engineering. *Tissue Eng Part C Methods*. 2013;19(11):885-891.



45. Osterhoff G, Löffler S, Steinke H, Feja C, Josten C, Hepp P. Comparative anatomical measurements of osseous structures in the ovine and human knee. *Knee*. 2011;18(2):98-103.
46. Pape D, Madry H. The preclinical sheep model of high tibial osteotomy relating basic science to the clinics: standards, techniques and pitfalls. *Knee Surg Sports Traumatol Arthrosc*. 2013;21(1):228-236.
47. Pridie KH. A method of resurfacing osteoarthritic knee joints: proceedings of the British Orthopaedic Association. *J Bone Joint Surg Br*. 1959;41:618-619.
48. Saris DB, Vanlauwe J, Victor J, et al. Treatment of symptomatic cartilage defects of the knee: characterized chondrocyte implantation results in better clinical outcome at 36 months in a randomized trial compared to microfracture. *Am J Sports Med*. 2009;37(suppl 1):10-19.
49. Sellers RS, Peluso D, Morris EA. The effect of recombinant human bone morphogenetic protein-2 (rhBMP-2) on the healing of full-thickness defects of articular cartilage. *J Bone Joint Surg Am*. 1997;79(10):1452-1463.
50. Shah SS, Lee S, Mithoefer K. Next-generation marrow stimulation technology for cartilage repair: basic science to clinical application. *JBJS Rev*. 2021;9(1):e20.00090.
51. Shapiro F, Koide S, Glimcher MJ. Cell origin and differentiation in the repair of full-thickness defects of articular cartilage. *J Bone Joint Surg Am*. 1993;75(4):532-553.
52. Shirazi R, Shirazi-Adl A, Hurtig M. Role of cartilage collagen fibrils networks in knee joint biomechanics under compression. *J Biomech*. 2008;41(16):3340-3348.
53. Smilie IS. Treatment of osteochondritis dissecans. *J Bone Joint Surg Br*. 1957;39(2):248-260.
54. Smith PK, Krohn RI, Hermanson GT, et al. Measurement of protein using bicinchoninic acid. *Anal Biochem*. 1985;150(1):76-85.
55. Steadman JR, Rodkey WG, Rodrigo JJ. Microfracture: surgical technique and rehabilitation to treat chondral defects. *Clin Orthop Relat Res*. 2001;391(suppl):362-369.
56. Utsunomiya H, Gao X, Cheng H, et al. Intra-articular injection of bevacizumab enhances bone marrow stimulation-mediated cartilage repair in a rabbit osteochondral defect model. *Am J Sports Med*. 2021;49(7):1871-1882.
57. Widuchowski W, Widuchowski J, Trzaska T. Articular cartilage defects: study of 25,124 knee arthroscopies. *Knee*. 2007;14(3):177-182.